



# Transmission of sodium chloride in PDMS membrane during Pervaporation based on polymer relaxation

Chengye Zuo<sup>a,b</sup>, Shuainan Xu<sup>a</sup>, Xiaobin Ding<sup>c</sup>, Wanqin Jin<sup>a</sup>, Weihong Xing<sup>a,\*\*</sup>, Xuebin Ke<sup>b,\*</sup>

<sup>a</sup> National Engineering Research Center for Special Separation Membranes, Nanjing Tech University, Nanjing, 211816, China

<sup>b</sup> Department of Chemical Engineering, University of Hull, HU6 7RX, United Kingdom

<sup>c</sup> Nanjing Jiushi High-Tech Co., Ltd., Nanjing, 211816, Jiangsu, China

## ARTICLE INFO

### Keywords:

Salt rejection  
Isobutanol  
Polydimethylsiloxane membrane  
Pervaporation  
Polymer relaxation

## ABSTRACT

Polydimethylsiloxane (PDMS) composite membrane is used for treating pharmaceutical wastewater containing NaCl and solvent. In this study, the influence of feed concentrations of NaCl and isobutanol, process temperature and membrane microstructures on salt rejection are evaluated. Microstructures of PDMS membrane before and after separation are characterized by nuclear magnetic resonance (NMR), energy dispersive X-ray spectroscopy (EDS), scanning electron microscope (SEM), Fourier transform infrared spectroscopy (FTIR), X-ray diffraction (XRD) and Positron annihilation life-time spectroscopy (PALS). The PV results show that NaCl will not spontaneously enter PDMS membrane without isobutanol. However, while NaCl feed concentration is 13 wt%, salt rejection of PDMS membrane drops from 100% to 99.09% with increasing feed concentration of isobutanol (up to 7 wt%). On the contrary, a higher temperature increases salt rejection of PDMS membrane and NaCl permeation through PDMS membrane is not through a vapor permeate process. Due to the relaxation of PDMS polymer chain, when PDMS cross-linking ratio is 0.1, the salt rejection increases from 99.87% to 100% with its thickness increasing from 10  $\mu\text{m}$  to 17.5  $\mu\text{m}$ . While the cross-linking ratio rises to 0.2, the salt rejection is 100% with the PDMS layer thickness of 10  $\mu\text{m}$ . The relationship between relaxation of polymer chains and transport of NaCl in PDMS membrane is an excellent guidance and will be beneficial for the treatment of saline organic wastewater.

## 1. Introduction

Wastewater recycling use is one of the key concerns in global environment [1,2]. Pharmaceutical wastewater contains large amounts of salts and organic solvents, such as NaCl ( $\leq 15$  wt%) and isobutanol ( $\leq 7$  wt%), which poses a serious threat to the environment and human health [3,4]. Therefore, NaCl removal and isobutanol recovery are essential demands to treat wastewater. Compared with traditional distillation technology, membrane process has higher efficiency and energy-saving potential [5]. Reverse osmosis (RO) is currently the most mature pressure-driven membrane process for desalination and the cost is relatively low [6]. Non-pressure-driven membrane processes, such as membrane distillation (MD) and Pervaporation (PV), are also attractive in the treatment of wastewater with dissolved solids, and have a strong resistance to fouling [7]. In addition, there has been many researches on separation and recovery of organics from water in the PV process [8,9].

Compared with other membrane technologies, PV has a great potential in the treatment of aqueous solutions containing NaCl and isobutanol.

PV is considered an economical and green separation process, in which specific components in feed preferentially dissolve and permeate through the dense membrane, then evaporate in downstream. There is a chemical potential gradient between feed side and permeate side of the composite membrane during PV, thereby creating a mass transfer driving force for the permeate [9–11]. Pervaporation membranes are generally dense, including hydrophilic or organophilic materials. Polyvinyl alcohol (PVA) [12], graphene oxide (GO) [13], mxene [11] and other two-dimensional hydrophilic materials have been used in pervaporation desalination, salt rejection for high-concentration saline wastewater can reach 99.99%–100% [14,15]. Apart from its emerging application in desalination, PV has been extensively used for liquid separations, such as dehydration of organic solvents, evaporation of volatile organics from aqueous solutions, and separation of organic

\* Corresponding author.

\*\* Corresponding author.

E-mail addresses: [xingwh@njtech.edu.cn](mailto:xingwh@njtech.edu.cn) (W. Xing), [x.ke@hull.ac.uk](mailto:x.ke@hull.ac.uk) (X. Ke).

<https://doi.org/10.1016/j.memsci.2022.120812>

Received 12 May 2022; Received in revised form 6 July 2022; Accepted 8 July 2022

Available online 16 July 2022

0376-7388/© 2022 The Authors. Published by Elsevier B.V. This is an open access article under the CC BY-NC-ND license (<http://creativecommons.org/licenses/by-nc-nd/4.0/>).

mixtures [8,9]. As a typical organophilic material, polydimethylsiloxane (PDMS) is widely used to recover organics in water due to its easy preparation and low cost. Therefore, it has extensive researches on the separation mechanism of binary or multi-system solvent systems [16, 17].

As the actual system contains not only organics but also a large quantity of soluble salt, researchers consequently study influence of salt on PV performance. At 35 °C–40 °C, PDMS-based composite membranes with different thicknesses are used to treat saline organic wastewater, including NaCl/n-butanol/water [18], NaCl/acetonitrile/water [19], ammonium sulfate/n-butanol/water [20,21]; As the feed concentration of salt increases, it can promote separation of organics from water due to the salting-out effect. But these separation processes did not explore the distribution of salt inside composite membranes. They claimed that salt does not pass through the functional layer of PDMS membrane as NaCl is not on the permeate side [22].

Furthermore, other researchers had systematically explored the distribution of salt in composite membranes based on silicone rubber. Through X-ray photoelectron spectroscopy (XPS), NaCl could be found in the membrane surface at the feed side [23]. Moreover, the theory of fouling on the membrane surface was proposed based on decreasing flux [24]. It partly explains the salt exists as hydrated ions in feed will increase the affinity between salt and silicone-based membrane [25]. On the whole, NaCl as an impermeable component, exists in a state of hydrated ions and is impossible to pass through a dense and defect-free PV membrane [11]. However, the organics were found to change the microstructure of PDMS polymer chain inferred from the solution-diffusion model [26], thus hydrated ions may pass through the PDMS layer and crystallize on permeate side. In fact, we did observe NaCl crystals on permeate side of PDMS membranes, when treating saline organic wastewater in PV (Fig. S1 for details).

In this work, concentration of isobutanol/NaCl and temperature in feed are investigated to explore their influence on the salt rejection of PDMS membrane. Microstructures of PDMS membrane before and after separation are characterized by nuclear magnetic resonance (NMR), energy dispersive X-ray spectra (EDS), scanning electron microscope (SEM), Fourier transform infrared spectroscopy (FTIR) and X-ray diffraction (XRD). Moreover, the thickness and crosslinking degree of PDMS membrane are investigated to explore the influence of the membrane microstructure on the rejection of NaCl. The purpose is to study the mechanism of NaCl passing through the PDMS membrane and establish the relationship between relaxation of polymer chains and salt rejection.

## 2. Materials and methods

### 2.1. Materials

All materials and reagents were commercial products (analytical grade) and used without further purification. Isobutanol and NaCl were from Sinopharm Chemical Co. Ltd., China. PDMS flat composite membranes were produced by Nanjing Jiushi High-Tech Co., Ltd., China [27]. The membrane consists of PDMS top layer with different thickness and crosslinking ratio, polyvinylidene fluoride (PVDF) intermediate layer with mean pore size of 76 nm and non-woven fabrics substrate layer. In addition, the thickness of PDMS layer (crosslinking ratio of TEOS: PDMS = 0.1) was determined by height of drawknife, therefore named PDMS, PDMS<sub>1</sub>, PDMS<sub>2</sub>, PDMS<sub>3</sub>, PDMS<sub>4</sub> from low to high [28]; the crosslinking ratio is controlled by TEOS: PDMS = 0.08 or 0.09 or 0.1 or 0.15 or 0.2 (PDMS layer thickness is consistent), it was therefore named PDMS<sub>0.08</sub>, PDMS<sub>0.09</sub>, PDMS<sub>0.1</sub>, PDMS<sub>0.15</sub>, PDMS<sub>0.2</sub> [29]. The surface properties of various PDMS composite membranes are shown in Fig. S2a and Fig. S2b.

### 2.2. Characterization

The morphology of membranes was observed by SEM (Hitachi S-

4800) at an acceleration voltage of 2 kV. An energy spectrum analysis system was used to analyze element distribution. Crystal structures of PDMS composite membranes were acquired by XRD (RIGAKU MiniFlex 600) using Cu K $\alpha$  radiation ( $\lambda = 0.154$  nm) with the range of 5–40° and an increment of 0.02°. ATR-FTIR spectra (Thermo Nicolet Nexus 470) were recorded in the range of 500–4000 cm<sup>-1</sup> to measure the surface properties.

The nuclear magnetic resonance technology (LF-NMR, NM42-40H-I) was used to measure the influence of solvents on relaxation of PDMS polymer chains [30]. The free-support dense PDMS membranes were immersed in 13 wt% NaCl/water and 13 wt% NaCl/1-7 wt% isobutanol/water to reach a swelling equilibrium. Subsequently, a slice of membranes (1 cm in diameter, 0.1 g) was placed in the bottom of a 7 mL glass vial. Then the glass vial was sealed and placed into the analyzer coil to get the T<sub>2</sub> decay curve. The NMR parameters are shown in Table 1. Moreover, the decay curve was inverted to obtain the T<sub>2</sub> relaxation spectrum through Laplace transform, where the number of inversion data points was 200, the number of iterations was 5000, and the fitting error was 0.006.

Free volume property of composite membranes with different crosslinking ratios were analyzed by PALS (DPLS3000). The EG&G ORTEC fast/slow coincidence system with a resolution of 210 ps was used. Then the spectrum was resolved by LTV9.0 software. The positron source (<sup>22</sup>Na, 7 × 10<sup>5</sup> Bq) was placed between two membrane samples (1 cm × 1 cm). Moreover, radius of free volume cavities ( $r_3$ ) and fractional free volume ( $f_{app}$ ) were obtained by Eqs. (1) and (2) [31,32].

$$\tau_3 = \frac{1}{2} \left[ 1 - \frac{r_3}{r_3 + \Delta r} + \left( \frac{1}{2\pi} \right) \sin \left( \frac{2\pi r_3}{r_3 + \Delta r} \right) \right]^{-1} \quad (1)$$

$$f_{app} = \frac{4\pi}{3} r_3^3 I_3 \quad (2)$$

where  $\tau_3$  is the ortho-positronium (o-Ps) pick-off lifetime;  $I_3$  is the corresponding intensity of o-Ps;  $\Delta r$  is the electron layer of thickness (0.1656 nm).

### 2.3. Swelling experiments

The homogeneous PDMS<sub>0.08</sub> composite membrane without support layer was used for swelling experiments to avoid the influence of the support. Typically, it is placed in a vacuum drying oven at 60 °C for 24 h before soaking, and then weigh it with a precision balance to obtain the dry membrane mass ( $W_1$ ). Membranes of known weight were soaked in 30 wt% NaCl/water and 30 wt% NaCl/5 wt% isobutanol/water. After a given period of time, take it out and use a dust-free cloth to dry the membrane surface solution quickly and carefully. PDMS<sub>0.08</sub> composite membranes are weighed to obtain the swollen homogeneous membrane mass at this time, and then put back into solution. Repeat the operation until the homogeneous membranes does not gain any further weight, and the mass ( $W_2$ ) of the membranes at this time is the swelling limit. Put the swollen composite membrane in an oven at 60 °C for 24 h, then weigh to get the mass ( $W_3$ ).

Swelling degree ( $S_1$ ) of the homogeneous PDMS<sub>0.08</sub> composite membrane is calculated by Eq. (3):

$$S_1 = \frac{W_2 - W_1}{W_1} \quad (3)$$

Salt in membrane ( $S_2$ ) is calculated by Eq. (4):

$$S_2 = \frac{W_3 - W_1}{W_1} \quad (4)$$

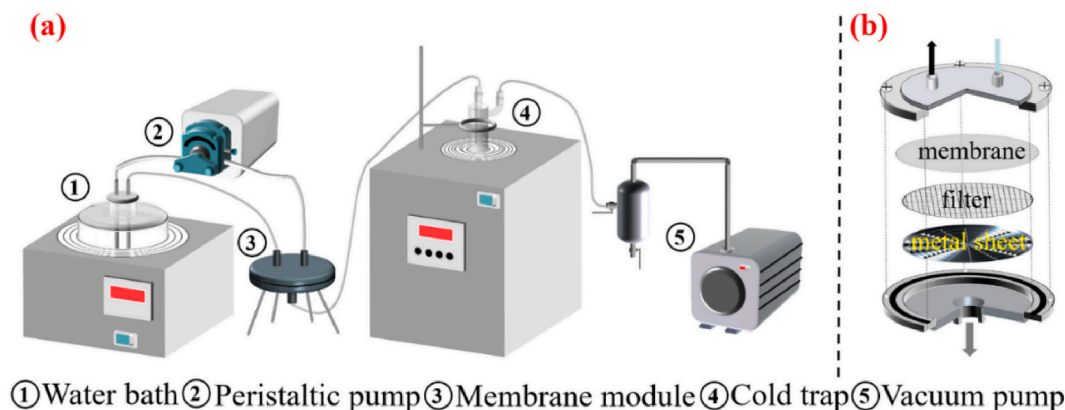
### 2.4. Pervaporation

The diagram of the experimental devices is shown in Fig. 1. Its equipment is set similar to the previous work [27], including heating

**Table 1**

NMR specific parameters.

magnetic	sampling number	sampling frequency	wait time	Rf delay	Analog gain	Digital Gain	cumulative frequency	echo time	number of echo
42.14 MHz	80,000	100 kHz	2000 m s	0.29 m s	20 db	3	4	0.08 m s	10,000

**Fig. 1.** (a) Experimental device diagram, (b) Plate membrane module.

system (water bath and feed tank), membrane module (membrane area is 153.86 cm<sup>2</sup>), cold trap, vacuum pump. Moreover, the peristaltic pump allows tangential flow through membrane module at a rate of 68 L·h<sup>-1</sup> (Reynolds≈253.8). The target components on permeate side of membranes are collected in a refrigerator cooling system (-70 °C) with a vacuum pump (150 Pa). The concentration of isobutanol in permeate is oversaturated, so it is necessary to dilute it 10 times before analysis using gas chromatograph (GC). All experimental results were repeated at least three times, an error of <5%. The feed liquid for each experiment was 1.2 L, and was preheated for half an hour. Every half an hour, we took samples for analysis. The concentration of isobutanol and NaCl in feed tank were 0–7 wt% and 0–13 wt%, respectively. The temperature of the feed liquid is 30–60 °C.

Mass transfer of NaCl in the PDMS composite membrane is indicated by the salt rejection ( $R$ ), and measured by indirect method [33], as Eq. (5):

$$R = \left(1 - \frac{m_s}{m \times C_f}\right) \times 100\% \quad (5)$$

where  $m_s$  is the weight of NaCl crystals on filter and metal sheet(g), as shown in Fig. 1b;  $m$  is the weight of liquid on the permeate (g); and  $C_f$  is the concentration of NaCl on the feed (wt%). It is worth noting that if only liquid evaporation occurs during PV, its theoretical salt rejection should be 100% [11]. However, it can be known that the components enter PDMS layer in a liquid state inferred from the series resistance model, and then vaporize in porous support [27]. Consequently, the hydrated ions of NaCl may pass through the PDMS layer and then crystallize in porous support.

Transmission of water and isobutanol in PDMS composite membrane are usually indicated as the flux  $J_i$ , determined by Eq. (6):

$$J_i = \frac{m_i}{A \times t} \quad (6)$$

where  $m_i$  is the mass of component  $i$  in the permeate (g);  $A$  is the effective membrane area (m<sup>2</sup>); and  $t$  is the run time for the PV (hour).

Long-term stability: Adopt PDMS<sub>4</sub> and PDMS<sub>0.2</sub> composite membranes to separate saline organic wastewater while feed concentration is 13 wt% NaCl and 1 wt% isobutanol at 40 °C. PV time was 8 hours, and the cycle run was 5 times. The variations of isobutanol mass concentration in feed was measured by GC, and salt rejection of two types composite membranes were calculated by indirect method.

### 3. Results and discussion

#### 3.1. Swelling of PDMS membrane in pure solvent

To check whether NaCl spontaneously enters the PDMS membrane layer, we test the swelling degree and the results are shown in Table 2. The homogeneous PDMS membrane without support did not swell obviously in 30 wt% NaCl aqueous solution, and the performance of PDMS membrane did not change after drying. It comes to a conclusion that NaCl did not enter the membrane. In addition, although the homogeneous PDMS membrane swelled in 30 wt% NaCl/5 wt% isobutanol aqueous solution, there was no significant weight gain after the membrane dried. Therefore, NaCl would not spontaneously enter the PDMS membrane.

#### 3.2. PV performance of PDMS composite membrane

##### 3.2.1. Influence of feed concentrations of NaCl and isobutanol

During pervaporation, the concentration of the components in feed will greatly affect their dissolution and diffusion processes in PDMS composite membrane [34,35]. Moreover, it can be seen from Section 3.1 that NaCl will not spontaneously enter the PDMS membrane, but chemical potential of components varies during the membrane PV. Therefore, the influence of feed concentrations of NaCl and isobutanol on flux and salt rejection are studied. Fig. 2a depicts that when isobutanol concentration is 7 wt% in feed and NaCl concentration increases from 1 wt% to 13 wt%, water flux gradually decreases and isobutanol flux gradually increases. This phenomenon is due to the salting-out effect: NaCl combines with free water to form hydrated ions, reducing the content of free water and thermodynamic activity [36]. As the free water for dissolving isobutanol decreases, the increase in activity of isobutanol leads to an increase in its mass transfer driving force and isobutanol flux. This is similar to the tendency of NaCl to promote the separation of

**Table 2**  
Swelling degree and salt in membrane of PDMS<sub>0.08</sub>.

System	Swelling degree (S <sub>1</sub> )/%	Salt in membrane (S <sub>2</sub> )/%
30 wt% NaCl/water	0.71 ± 0.33	(9.56 ± 0.27)E <sup>-2</sup>
30 wt% NaCl/5 wt% isobutanol/water	9.44 ± 0.01	(5.46 ± 0.01)E <sup>-2</sup>

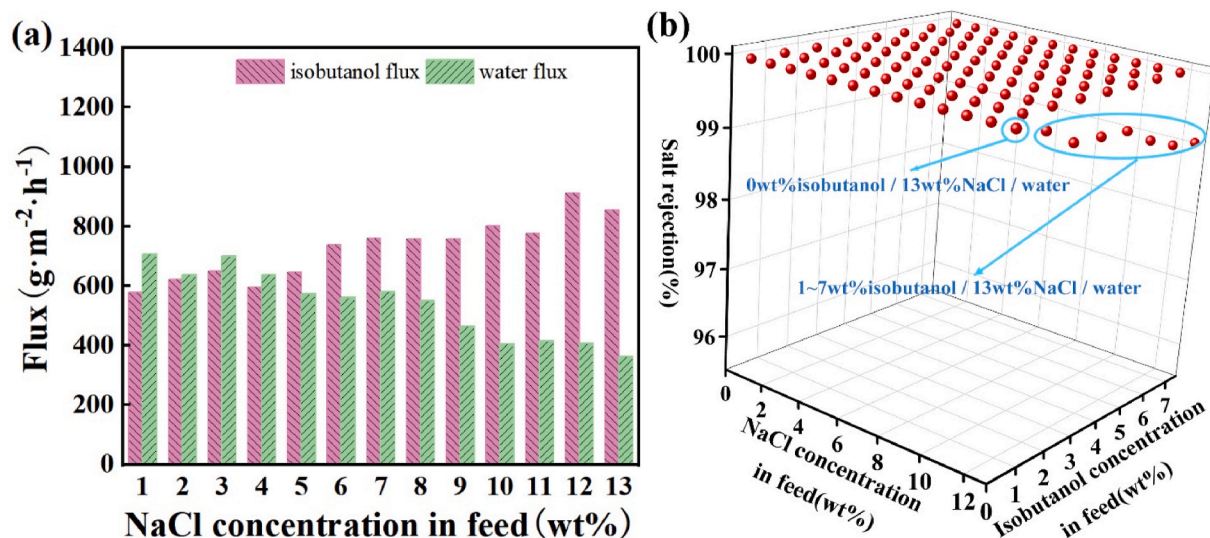


Fig. 2. Effect of feed concentration in NaCl/butanol/water ternary system on (a) flux (7 wt% isobutanol) and (b) salt rejection of PDMS membrane (feed temperature: 40 °C).

n-propanol in water with composite membrane [23]. Moreover, the size of hydrated ions of NaCl is much larger than that of water molecules, therefore reducing mass transfer and resulting in negative impact on water flux [19].

Fig. 2b describes the combined effect of feed concentrations of NaCl and isobutanol on salt rejection of PDMS membrane. When the isobutanol concentration is 1 wt% and NaCl concentration increases to 13 wt%, the salt rejection of PDMS membrane drops to 99.87%. This is due to that maximum hydration number in first hydration shell of sodium ions is five. When more free water is added, a second, higher-level hydration shell will be formed [37]. Sodium ions are more likely to form  $\text{Na}^+\cdot 1\sim 5\text{H}_2\text{O}$ , and they have a smaller radius of gyration (list in Table 3). At the same time, the composite membrane swells in isobutanol and causes the free volume of the PDMS polymer chain to increase [38], eventually resulting in a decrease in salt rejection of PDMS membrane.

Fig. 2b shows while NaCl concentration reaches 13 wt% and isobutanol concentration increases from 0 wt% to 1 wt%, salt rejection of PDMS membrane drops from 100% to 99.87%. The high isobutanol concentration increases swelling of PDMS membrane and leads to changes in the microstructure of PDMS polymer chain [30]. The swelling behavior of PDMS in isobutanol could be identified by the spin-spin relaxation times ( $T_2$ ), which was measured in NMR. The higher  $T_2$  indicates a larger free space in the membrane, which is attributed to an increase in degree of polymer chain relaxation [30,39]. Fig. 3 depicts that the relaxation times inversion spectra of polymer network,  $T_{2s}$  and  $T_{2m}$ . On the one hand,  $T_{2s}$  corresponded to protons of the polymer chains close to the crosslinking site. On the other hand,  $T_{2m}$  corresponds to a proton of the polymer chain located in the network while being indirectly attached to the cross-linker site [40]. As the isobutanol concentration in feed gradually increased, there was no significant changes on  $T_{2s}$ , but increased the  $T_{2m}$  of PDMS. It suggests the swelling (by isobutanol) should increase the movement of polymer chain between the cross-linking sites, thereby increasing relaxation of PDMS and reducing the salt rejection of PDMS membrane.

Table 3  
Radius of gyration of hydrate ions [37].

hydration number	$\text{Na}^+\cdot 1\text{H}_2\text{O}$	$\text{Na}^+\cdot 2\text{H}_2\text{O}$	$\text{Na}^+\cdot 3\text{H}_2\text{O}$	$\text{Na}^+\cdot 4\text{H}_2\text{O}$	$\text{Na}^+\cdot 5\text{H}_2\text{O}$
radius of gyration	0.375 nm	0.515 nm	0.56 nm	0.565 nm	0.61 nm

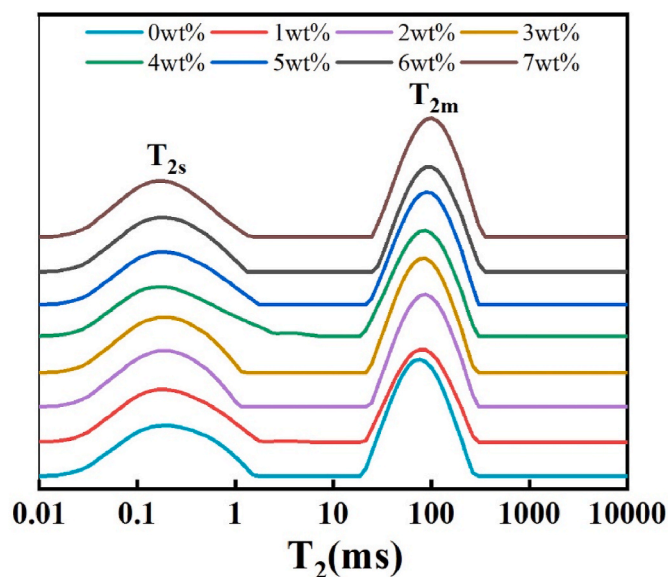


Fig. 3. Comparison of the relaxation times of PDMS<sub>0.1</sub> in 13 wt% NaCl/0 wt% - 7 wt% isobutanol/water.

In order to investigate the distribution and mass transfer of NaCl in PDMS membrane, the elements, morphology, surface properties and structure of PDMS membrane before and after separation are analyzed. As shown in Fig. 4a and Fig. 4b, NaCl is shown in the transition layer, base membrane layer and the permeate side. It is preliminarily determined that NaCl permeation through PDMS membrane is a dissolution-recrystallization process. Moreover, Fig. S5a and Fig. S5b show that there is no NaCl inside the PDMS composite membrane when the salt rejection is 100%. However, when 7 wt% isobutanol is present in the system, sodium chloride is distributed inside the substrate. Fig. 4c and d depict that the surface properties and crystal structure of PDMS membrane have not significantly changed before and after separation. Moreover, PDMS membrane can maintain 100% salt rejection when repeatedly treating 13 wt% NaCl in water (Table S1 for details). Therefore, it can be concluded that NaCl can pass through PDMS membrane under certain feeding conditions and PDMS membrane microstructure did not change during this process.

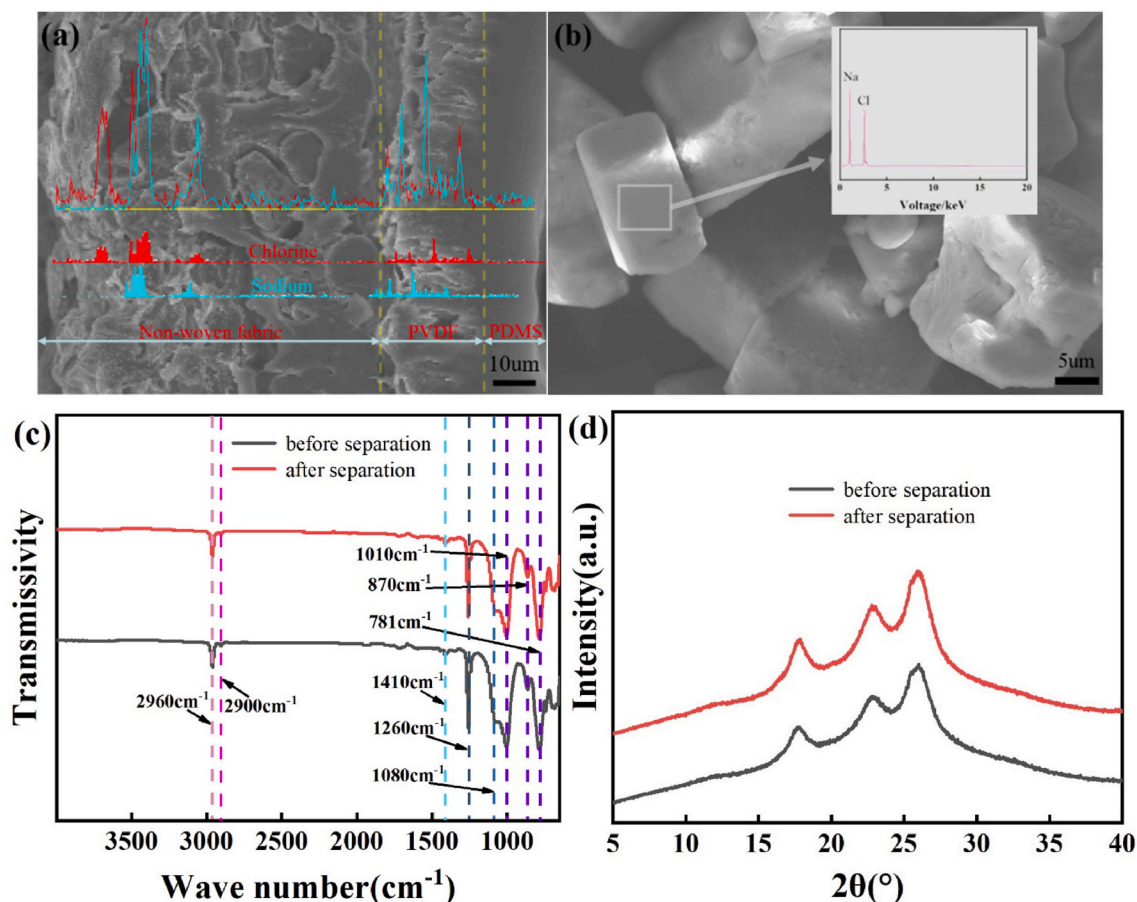


Fig. 4. Element distribution of (a) membrane cross section (13 wt% NaCl/1 wt% isobutanol/water), (b) crystals on PDMS membrane permeate side; (c) Infrared spectra and (d) XRD pattern of PDMS membrane before and after separation.

### 3.2.2. Effect of feed temperature

Temperature is an important factor for the transport of components in PDMS composite membrane during PV. It not only affects the dissolution and diffusion of isobutanol, but also increases thermal motion of PDMS polymer chain, lead to increase its free volume [14]. Combine with section 3.2.1 that decrease in PDMS salt rejection is caused by increase in relaxation of PDMS polymer chain. Thus, the effect of feed temperature is investigated under the isobutanol and NaCl concentrations of 1 wt% and 13 wt%, respectively. It can be found in Fig. 5 that water flux and isobutanol flux gradually increase as the temperature rises from 30 °C to 60 °C. This is because temperature increases thermal

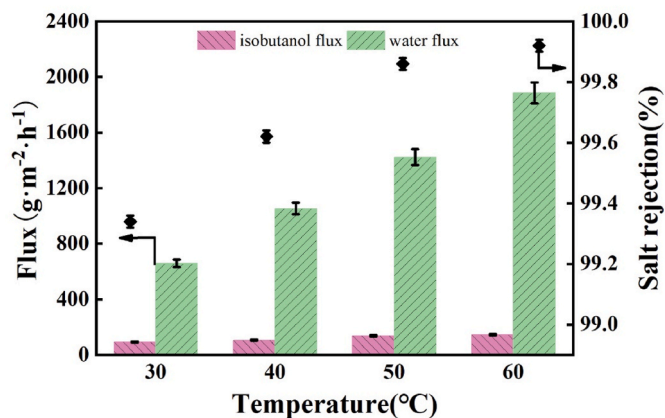


Fig. 5. Effect of feed temperature on flux and salt rejection (feed composition: 1 wt% isobutanol and 13 wt% NaCl in water).

movement of components, and also increases the swing of PDMS polymer chain, which promotes penetration of components [41]. In addition, temperature rise will increase diffusivity of hydrated ions [29,42], but it is found from Fig. 5 that PDMS membrane salt rejection rises from 99.34% to 99.92% with the rise of temperature. Table 1 shows that hydrated ion cannot be dissolved in PDMS, which makes its resistance to passing through PDMS membrane remarkably. Therefore, the polymer chain caused by temperature cannot increase the NaCl transport, and the relaxation of the PDMS polymer chain caused by isobutanol is a key factor for reduction of PDMS salt rejection.

### 3.2.3. Influence of PDMS layer thickness

The thinner thickness of PDMS layer, the more likely it is to aggregate polymer chains, resulting in a looser structure of the polymer chains [43]. In addition, Section 3.2.2 shows that the passage of NaCl through the PDMS polymer membrane is attributed to the swelling and relaxation of the polymer chain, which provides a transport channel for hydrated ions. Composite membranes with different PDMS layer thicknesses were prepared to treat 13 wt% NaCl/1 wt% isobutanol/water system. As shown in Fig. 6, PDMS composite membranes were prepared with thicknesses of 10 μm, 11.3 μm, 13.2 μm, 14.8 μm, and 17.5 μm.

Fig. 7 depicts the effect of the PDMS layer thickness on salt rejection and each component flux. As shown in Fig. 7a, the composite membranes have a characteristic peak near 2θ = 12°, which corresponds to the PDMS tetragonal lattice reported in the literature [44]. Due to the solvent-induced crystallization [45], thicker polymer chains have enough time to arrange into new crystallites in n-heptane, resulting in crystallinity of PDMS gradually increases with increasing thickness. The

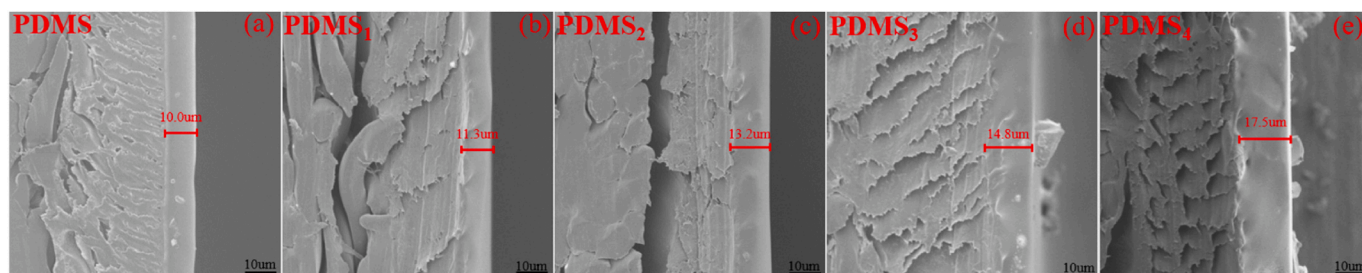


Fig. 6. SEM cross-section images of PDMS membranes with different thicknesses.

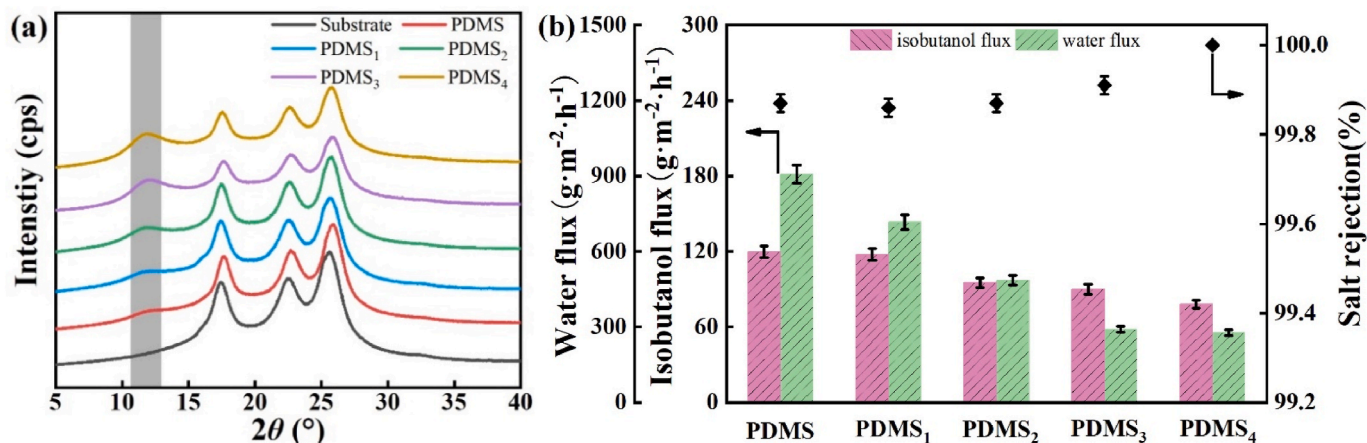


Fig. 7. Effect of PDMS membranes thicknesses on (a) XRD patterns, (b) flux and salt rejection (feed composition: 1 wt% isobutanol and 13 wt% NaCl in water, feed temperature: 40 °C).

composite membrane with a higher thickness has better anti-swelling [46]. In addition, the mean square radius of gyration and linear density of PDMS polymer chains increase with the increase of its layer thickness [43]. Therefore, Fig. 7b shows that as PDMS layer thickness increases from 10  $\mu\text{m}$  to 17.5  $\mu\text{m}$ , water flux and isobutanol flux gradually decrease due to resistance brought by the thickness, and salt rejection of composite membrane gradually increased. Permeability was used to exclude the influence of PDMS thickness (Fig. S3 for detail). It can be found that water permeability and water flux have the same trend with thickness. In addition, PDMS layer thickness reaches 17.5  $\mu\text{m}$ , the mass transfer resistance of the composite membrane to hydrated ions is infinite, and the composite membrane salt rejection rate reaches 100% at this time.

### 3.2.4. Influence of PDMS layer cross-linking ratio

According to Section 3.2.3 that increasing strength of polymer chain can effectively reduce hydrated ions to pass through PDMS membrane. The strength of PDMS polymer chain can be also enhanced by increasing extent of cross-linking, thereby reducing the degree of swelling on it by organic solvents [47]. In addition, higher degree of cross-linking

restricts on the free space between the polymer chains and results in its lower relaxation [48]. As shown in Fig. 8, the crosslinking ratio of PDMS layer was changed to prepare membranes with about 10  $\mu\text{m}$  thickness. The membrane interfaces are well bonded and used to treat 13 wt% NaCl/1 wt% isobutanol/water system.

Fig. 9a shows that as crosslinking ratio increases, the swelling degree of PDMS membrane gradually decreases. This is owing to the increased degree of cross-linking restricting the movement of polymer chains.

The microstructure of PDMS layers with cross-linking ratios of 0.08 and 0.2 are observed by PLAS (Fig. S4 for detail), and the free volume between PDMS polymer chains is calculated by Eq. (2) and Eq. (3), as shown in Table 4. When crosslinking ratio is 0.08, free volume of PDMS polymer chain is 10.792. While crosslinking ratio increases to 0.2, its free volume decreases by 1.7%. Xie et al. found that diffusion of NaCl in PVA composite membrane is limited by free volume of polymer [49]. Therefore, as cross-linking ratio increases, the resistance of PDMS membrane to hydrated ions gradually increases, and shown in Fig. 9b, PDMS membrane salt rejection reaches 100% when cross-linking ratio is 0.2. The water flux and isobutanol flux in Fig. 9b gradually decrease with increasing resistance, same as in literature [29]. In conclusion, free

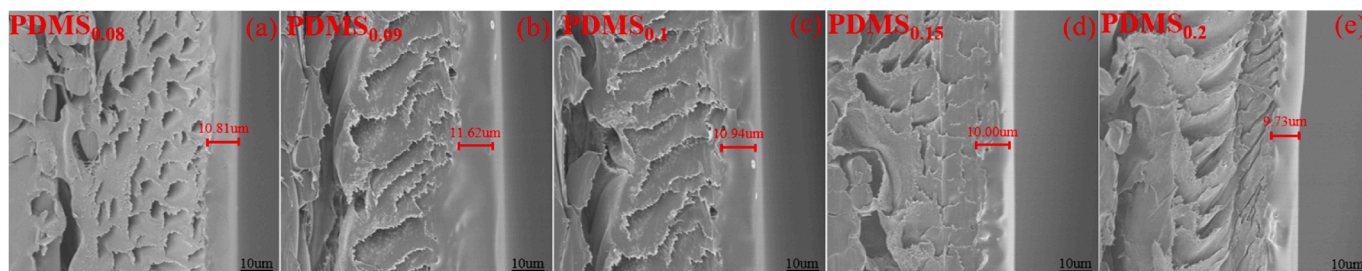


Fig. 8. Cross-sectional SEM images of PDMS membranes with different crosslinking ratio (TEOS: PDMS = 0.08:1, 0.09:1, 0.1:1, 0.15:1, 0.2:1).

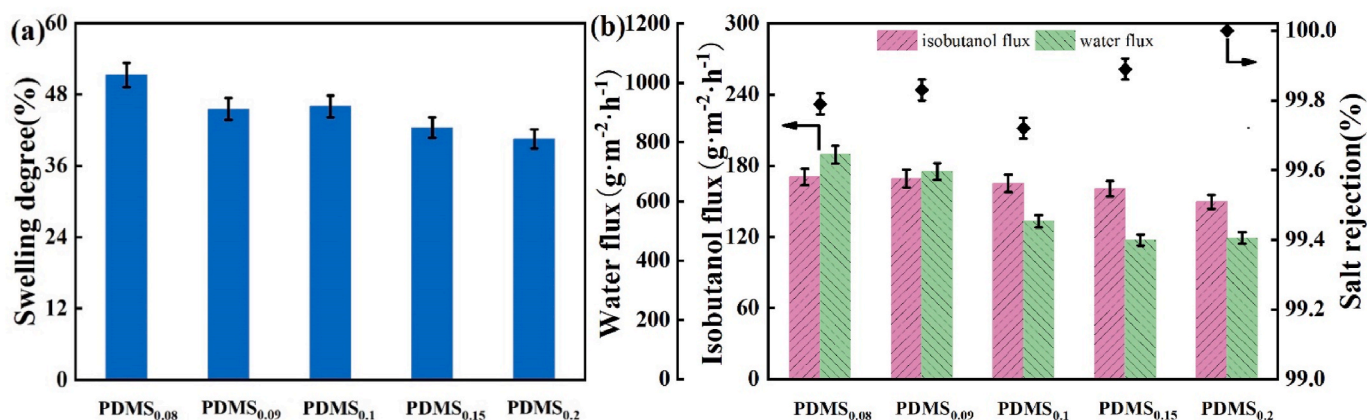


Fig. 9. Effect of PDMS membranes with different crosslinking ratio on (a) swelling degree, (b) flux and salt rejection (feed composition: 1 wt% isobutanol and 13 wt% NaCl in water, feed temperature: 40 °C).

Table 4

Free volume property of the PDMS<sub>0.08</sub> and PDMS<sub>0.2</sub>.

Membrane	$I_3$ (%)	$\tau_3$ (ns)	$r_3$ (nm)	$f_{app}$
PDMS <sub>0.08</sub>	45.5	3.352	0.384	10.792
PDMS <sub>0.2</sub>	43.9	3.361	0.387	10.609

volume change between polymer chains in PDMS layer is crucial for hydrated ions pass through.

### 3.2.5. Long-term stability

Fig. 10 describes the variations of isobutanol concentration in feed and salt rejection with the long-term test of 40 h (cycle 5 times). At 40 °C, PDMS<sub>4</sub> and PDMS<sub>0.2</sub> are used for separating 1 wt% isobutanol and 13 wt% NaCl aqueous solution. It can be noticed that the salt rejection maintained at 100% during the 40 h continuously. Moreover, the isobutanol concentration in feed decreased gradually from 1 wt% to 0.3–0.4 wt%, indicating that these two types of PDMS composite membranes have stable separation performance.

## 4. Conclusions

The transport of NaCl in PDMS composite membrane is systematically investigated. NaCl cannot be dissolved in PDMS layer and its hydrated ions cannot spontaneously enter PDMS polymer chain. However, chemical potential gradient exists in PDMS membrane during PV, resulting in relaxation of PDMS polymer chain. Therefore, hydrated ions

of NaCl pass through PDMS membrane of 10  $\mu\text{m}$  thickness while a cross-linking degree is 0.1 and the aqueous solution contains 1 wt% isobutanol and 13 wt% NaCl.

The feed contains 13 wt% NaCl, the salt rejection of PDMS membrane gradually decreased when feed concentration of isobutanol increased from 0 wt% to 7 wt%. On the contrary, its salt rejection gradually increased as temperature rise from 30 °C to 60 °C. In addition, it is observed through EDS that NaCl is distributed in substrate, and crystal in permeate side is NaCl. The surface properties and microstructure of PDMS membrane before and after separation have not changed, which indicates the permeate of NaCl through PDMS layer is not a vapor permeate process.

By changing the thickness and cross-linking ratio of the PDMS layer, thereby varying its relaxation and free volume, the salt rejection of PDMS membrane can be effectively improved. When the cross-linking ratio and thickness of PDMS layer are 0.1 and 17.5  $\mu\text{m}$  or 0.2 and 10  $\mu\text{m}$ , respectively, the salt rejection can reach 100% in the separation of 13 wt% NaCl/1 wt% isobutanol/water. This study provides the potential for pervaporation process to treat saline organic wastewater, and may be applied to the separation of waste water with similar properties.

### CRedit author statements

Chengye Zuo: Conceptualization, Methodology, Investigation, Writing- Original draft preparation.

Shuainan Xu: Methodology, Investigation, Validation.

Xiaobin Ding: Resources, Investigation and project administration.

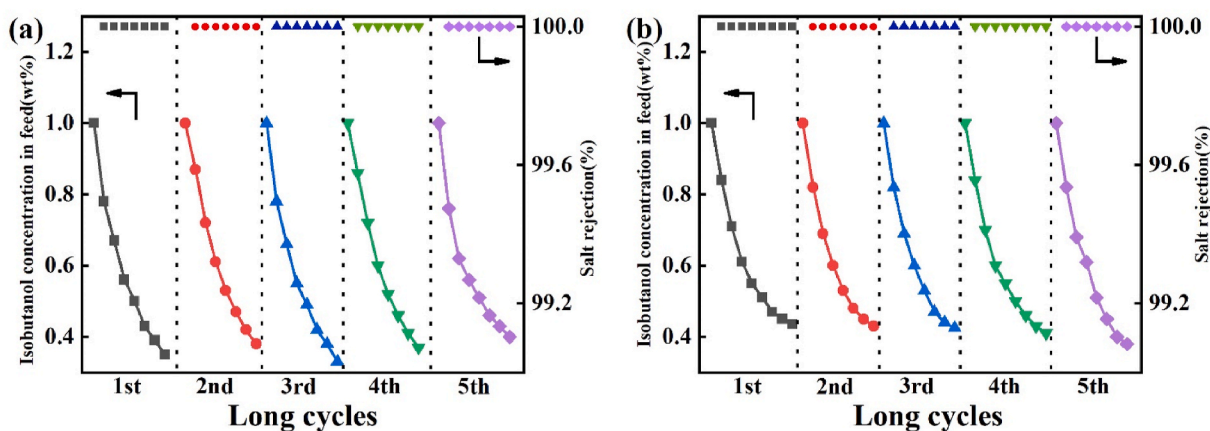


Fig. 10. Long-term stability and salt rejection of (a) PDMS<sub>4</sub>, (b) PDMS<sub>0.2</sub>. (feed composition: 1 wt% isobutanol and 13 wt% NaCl in water, feed temperature: 40 °C, cycle time: 8 h).

Wanqin Jin, Weihong Xing and Xuebin Ke: Conceptualization, Supervision, Writing- Reviewing and Editing.

All persons who meet authorship criteria are listed as authors, and all authors certify that they have participated sufficiently in the work to take public responsibility for the content, including participation in the concept, design, analysis, writing, or revision of the manuscript. Furthermore, each author certifies that this material or similar material has not been and will not be submitted to or published in any other publication before its appearance in the *Journal of Membrane Science*.

### Declaration of competing interest

The authors declare that they have no known competing financial interests or personal relationships that could have appeared to influence the work reported in this paper.

### Data availability

Data will be made available on request.

### Acknowledgement

This work is supported by the National Natural Science Foundation of China (No. 21921006). XK thanks the support of the THYME project (Research England) and British Academy grant (PPHE210322).

### Appendix A. Supplementary data

Supplementary data to this article can be found online at <https://doi.org/10.1016/j.memsci.2022.120812>.

### References

- P. Milillo, E. Rignot, P. Rizzoli, B. Scheuchl, J. Mouginot, J. Bueso-Bello, P. Prats-Iraola, Heterogeneous retreat and ice melt of thwaites glacier, west Antarctica, *Sci. Adv.* 5 (2019) u3433.
- S. Li, J. Chen, S. Hu, H. Wang, W. Jiang, X. Chen, Facile construction of novel Bi<sub>2</sub>WO<sub>6</sub>/Ta<sub>3</sub>N<sub>5</sub> Z-scheme heterojunction nanofibers for efficient degradation of harmful pharmaceutical pollutants, *Chem. Eng. J.* 402 (2020).
- H.T. Luk, C. Mondelli, D.C. Ferre, J.A. Stewart, J. Perez-Ramirez, Status and prospects in higher alcohols synthesis from syngas, *Chem. Soc. Rev.* 46 (2017) 1358–1426.
- K. Wu, Y. Li, Solubility and solution thermodynamics of isobutyramide in 15 pure solvents at temperatures from 273.15 to 324.75 K, *J. Mol. Liq.* 311 (2020), 113294.
- J. Imbrogno, G. Belfort, Membrane desalination: where are we, and what can we learn from fundamentals? *Annu Rev Chem Biomol Eng* 7 (2016) 29–64.
- C. Charcosset, A review of membrane processes and renewable energies for desalination, *Desalination* 245 (2009) 214–231.
- E. Drioli, A. Ali, F. Macedonio, Membrane distillation: recent developments and perspectives, *Desalination* 356 (2015) 56–84.
- A. Rajawat, S. Subramanian, S. Ramakrishna, Progress on silica pervaporation membranes in solvent dehydration and solvent recovery processes, *Materials* 13 (2020) 3354.
- W.F. Yong, H. Zhang, Recent advances in polymer blend membranes for gas separation and pervaporation, *Prog. Mater. Sci.* 116 (2021), 100713.
- Y.K. Ong, G.M. Shi, N.L. Le, Y.P. Tang, J. Zuo, S.P. Nunes, T. Chung, Recent membrane development for pervaporation processes, *Prog. Polym. Sci.* 57 (2016) 1–31.
- G. Liu, J. Shen, Q. Liu, G. Liu, J. Xiong, J. Yang, W. Jin, Ultrathin two-dimensional MXene membrane for pervaporation desalination, *J. Membr. Sci.* 548 (2018) 548–558.
- B. Liang, Q. Li, B. Cao, P. Li, Water permeance, permeability and desalination properties of the sulfonic acid functionalized composite pervaporation membranes, *Desalination* 433 (2018) 132–140.
- L. Li, J. Hou, V. Chen, Pinning down the water transport mechanism in graphene oxide pervaporation desalination membranes, *Ind. Eng. Chem. Res.* 58 (2019) 4231–4239.
- Q. Wang, N. Li, B. Bolto, M. Hoang, Z. Xie, Desalination by pervaporation: a review, *Desalination* 387 (2016) 46–60.
- R. Castro-Muñoz, Breakthroughs on tailoring pervaporation membranes for water desalination: a review, *Water Res.* 187 (2020), 116428.
- N. Moriyama, Y. Kawano, Q. Wang, R. Inoue, M. Guo, M. Yokoji, H. Nagasawa, M. Kanezashi, T. Tsuru, Pervaporation via silicon-based membranes: correlation and prediction of performance in pervaporation and gas permeation, *AIChE J.* 67 (2021).
- P. Shao, R.Y.M. Huang, Polymeric membrane pervaporation, *J. Membr. Sci.* 287 (2007) 162–179.
- S. Yi, Y. Wan, Separation performance of novel vinyltriethoxysilane (VTES)-g-silicalite-1/PDMS/PAN thin-film composite membrane in the recovery of bioethanol from fermentation broths by pervaporation, *J. Membr. Sci.* 524 (2017) 132–140.
- Y. Wang, X. Mei, T. Ma, C. Xue, Y. Li, Green recovery of hazardous acetonitrile from high-salt chemical wastewater by pervaporation, *J. Clean. Prod.* 197 (2018).
- S. Chovau, S. Gaykawad, A.J.J. Straathof, B. Van der Bruggen, Influence of fermentation by-products on the purification of ethanol from water using pervaporation, *Bioresour. Technol.* 102 (2011) 1669–1674.
- E. Favre, Q.T. Nguyen, S. Bruneau, Extraction of 1-butanol from aqueous solutions by pervaporation, *J. Chem. Technol. Biotechnol.* 65 (1996) 221–228.
- W. Kujawski, S. Krajewski, Influence of inorganic salt on the effectiveness of liquid mixtures separation by pervaporation, *Separ. Purif. Technol.* 57 (2007) 495–501.
- F. Lipnizki, S. Hausmanns, R.W. Field, Influence of impermeable components on the permeation of aqueous 1-propanol mixtures in hydrophobic pervaporation, *J. Membr. Sci.* 228 (2004) 129–138.
- R. Martínez, M. Teresa Sanz, S. Beltrán, Concentration by pervaporation of brown crab volatile compounds from dilute model solutions: evaluation of PDMS membrane, *J. Membr. Sci.* 428 (2013) 371–379.
- C. Dotrémont, Pervaporation for the Removal of Chlorinated Hydrocarbons from Industrial Waste Water, Katholieke Universiteit Leuven, Belgium, 1994.
- J.G. Wijmans, R.W. Baker, The solution-diffusion model - a review, *J. Membr. Sci.* 107 (1995) 1–21.
- C. Zuo, J. Hindley, X. Ding, M. Gronnow, W. Xing, X. Ke, Transmission of butanol isomers in pervaporation based on series resistance model, *J. Membr. Sci.* 638 (2021), 119702.
- Y. Pan, Y. Hang, X. Zhao, G. Liu, W. Jin, Optimizing separation performance and interfacial adhesion of PDMS/PVDF composite membranes for butanol recovery from aqueous solution, *J. Membr. Sci.* 579 (2019) 210–218.
- R. Xu, G. Liu, X. Dong, W. Jin, Pervaporation separation of n-octane/thiophene mixtures using polydimethylsiloxane/ceramic composite membranes, *Desalination* 258 (2010) 106–111.
- C. Li, J. Li, W. Zhang, N. Wang, S. Ji, Q. An, Enhanced permeance for PDMS organic solvent nanofiltration membranes using modified mesoporous silica nanoparticles, *J. Membr. Sci.* 612 (2020).
- K. Cao, Z. Jiang, J. Zhao, C. Zhao, C. Gao, F. Pan, B. Wang, X. Cao, J. Yang, Enhanced water permeation through sodium alginate membranes by incorporating graphene oxides, *J. Membr. Sci.* 469 (2014) 272–283.
- Z. Si, D. Cai, S. Li, G. Li, Z. Wang, P. Qin, A high-efficiency diffusion process in carbonized ZIF-8 incorporated mixed matrix membrane for n-butanol recovery, *Separ. Purif. Technol.* 221 (2019) 286–293.
- Y.L. Xue, C.H. Lau, B. Cao, P. Li, Elucidating the impact of polymer crosslinking and fixed carrier on enhanced water transport during desalination using pervaporation membranes, *J. Membr. Sci.* 575 (2019) 135–146.
- G. Liu, W. Wei, H. Wu, X. Dong, M. Jiang, W. Jin, Pervaporation performance of PDMS/ceramic composite membrane in acetone butanol ethanol (ABE) fermentation-PV coupled process, *J. Membr. Sci.* 373 (2011) 121–129.
- V. Garcia, E. Pongracz, E. Muurinen, R.L. Keiski, Recovery of n-butanol from salt containing solutions by pervaporation, *Desalination* 241 (2009) 201–211.
- W. Kujawski, S. Krajewska, M. Kujawski, L. Gazagnes, A. Larbot, M. Persin, Pervaporation properties of fluoroalkylsilane (FAS) grafted ceramic membranes, *Desalination* 205 (2007) 75–86.
- J. Peng, D. Cao, Z. He, J. Guo, P. Hapala, R. Ma, B. Cheng, J. Chen, W.J. Xie, X. Li, P. Jelínek, L. Xu, Y.Q. Gao, E. Wang, Y. Jiang, The effect of hydration number on the interfacial transport of sodium ions, *Nature* 557 (2018) 701–705.
- Q. Zhu, B. Shentu, Q. Liu, Z. Weng, Swelling behavior of polyethylenimine-cobalt complex in water, *Eur. Polym. J.* 42 (2006) 1417–1422.
- V.M. Litvinov, A.A. Zhdanov, Role of various factors in the restriction of molecular mobility of polymer chains in filled polymers, *Polym. Sci* 30 (1988) 976–981.
- A. Azoug, A. Constantinescu, R. Nevière, G. Jacob, Microstructure and deformation mechanisms of a solid propellant using 1H NMR spectroscopy, *Fuel* 148 (2015) 39–47.
- S. Santoro, F. Galiano, J.C. Jansen, A. Figoli, Strategy for scale-up of SBS pervaporation membranes for ethanol recovery from diluted aqueous solutions, *Separ. Purif. Technol.* 176 (2017) 252–261.
- H. Sun, M. Yu, Z. Li, S. Almheiri, A molecular dynamic simulation of hydrated proton transfer in perfluorosulfonate ionomer membranes (nafion 117), *J. Chem.* 2015 (2015) 1–10.
- G.L. Jadav, V.K. Aswal, H. Bhatt, J.C. Chaudhari, P.S. Singh, Influence of film thickness on the structure and properties of PDMS membrane, *J. Membr. Sci.* 415–416 (2012) 624–634.
- L. Qu, G. Huang, Q. Wang, Z. Xie, Effect of diphenylsiloxane unit content on aggregation structure of poly(dimethylsiloxane-co-diphenylsiloxane), *J. Polym. Sci. B Polym. Phys.* 46 (2008) 72–79.
- H. Yang, Q.T. Nguyen, Y. Ding, Y. Long, Z. Ping, Investigation of poly(dimethyl siloxane) (PDMS)-solvent interactions by DSC, *J. Membr. Sci.* 164 (2000) 37–43.
- R. Ravindra, A. Kameswara Rao, A.A. Khan, Processing of liquid propellant reaction liquors by pervaporation, *J. Appl. Polym. Sci.* 72 (1999) 141–149.

- [47] N. Stafie, D.F. Stamatialis, M. Wessling, Effect of PDMS cross-linking degree on the permeation performance of PAN/PDMS composite nanofiltration membranes, *Separ. Purif. Technol.* 45 (2005) 220–231.
- [48] L. Huang, Y. Shui, W. Chen, Z. Li, H. Song, G. Sun, J. Xu, G. Zhong, D. Liu, How the aggregates determine bound rubber models in silicone rubber? A contrast matching neutron scattering study, *Chin. J. Polym. Sci.* 39 (2021) 365–376.
- [49] Z. Xie, M. Hoang, D. Ng, C. Doherty, A. Hill, S. Gray, Effect of heat treatment on pervaporation separation of aqueous salt solution using hybrid PVA/MA/TEOS membrane, *Separ. Purif. Technol.* 127 (2014) 10–17.